Acta Crystallographica Section D
Biological Crystallography
ISSN 0907-4449

Macromolecular neutron crystallography at the Protein Crystallography Station (PCS)

Andrey Kovalevsky,* Zoe Fisher, Hannah Johnson, Marat Mustyakimov, Mary Jo Waltman and Paul Langan

Bioscience Division, Los Alamos National Laboratory, Los Alamos, NM 87545, USA

Correspondence e-mail: ayk@lanl.gov

Received 30 April 2010
Accepted 8 July 2010

The Protein Crystallography Station (PCS) at Los Alamos Neutron Science Center is a high-performance beamline that forms the core of a capability for neutron macromolecular structure and function determination. Neutron diffraction is a powerful technique for locating H atoms and can therefore provide unique information about how biological macromolecules function and interact with each other and smaller molecules. Users of the PCS have access to neutron beam time, deuteration facilities, the expression of proteins and the synthesis of substrates with stable isotopes and also support for data reduction and structure analysis. The beamline exploits the pulsed nature of spallation neutrons and a large electronic detector in order to collect wavelength-resolved Laue patterns using all available neutrons in the white beam. The PCS user facility is described and highlights from the user program are presented.

1. Introduction

The Protein Crystallography Station (PCS) at Los Alamos National Laboratory is a high-performance neutron beamline operated by the Bioscience Division as a user facility for the Office of Biological and Environmental Research of the US Department of Energy (DOE). The successful construction and commissioning of the PCS at the spallation neutron source run by Los Alamos Neutron Science Center (LANSCE) by the end of 2002 was a major development for the field of neutron macromolecular crystallography for two main reasons. Firstly, whereas previous macromolecular neutron beamlines had been built at reactor neutron sources, the PCS was the first to be built at a spallation neutron source. The PCS was therefore an important proof-of-principle for the innovation of spallation macromolecular neutron crystallography, laying the ground for future beamlines that are currently under construction at more powerful next-generation spallation neutron sources throughout the world (Teixeira *et al.*, 2008). Secondly, the PCS was a much-needed addition to the relatively small pool of neutron beamlines that were available worldwide at the time to the structural biology community. Although this pool is now growing at an unprecedented rate, at present the PCS remains the only capability dedicated to neutron macromolecular crystallography in North America.

The construction and operation of the PCS required the development of several new technical and methodological approaches to protein crystallography because of the very different characteristics of spallation neutron sources compared with the reactor neutron sources on which previous macromolecular beamlines had been built (Langan *et al.*, 2004; Langan & Greene, 2004). In particular, the PCS exploits the pulsed nature of spallation sources and a large electronic

Table 1
Macromolecular structure determinations performed at the PCS.

Macromolecule	Unit-cell parameters (Å, °)	Space group	Resolution (Å)	Completeness (%)	Crystal volume (mm^3)	Collection duration (d)	PDB code	Citation
Rubredoxin, W3Y mutant	$a = 34.3, b = 35.3, c = 44.2$	$P2_12_12_1$	2.10	72	~2	5	—	Li *et al.* (2004)
Escherichia coli DHFR–methotrexate	$a = b = 93.1, c = 73.9$	$P6_1$	2.17	80	0.3	23	2inq	Bennett *et al.* (2006)
XI–$2Co^{2+}$	$a = 93.9, b = 99.7, c = 102.9$	$I222$	1.80	78	8	19	2gve	Katz *et al.* (2006)
Z-DNA, d(CGCGCG)	$a = 18.0, b = 31.2, c = 44.9$	$P2_12_12_1$	1.60	62	0.7	18	—	Langan *et al.* (2006)
PYP	$a = 66.8, b = 66.8, c = 41.0$	$P6_3$	2.50	89	0.8	14	2qws	Fisher *et al.* (2007)
Endothiapepsin–*gem*-diol inhibitor	$a = 43.0, b = 75.7, c = 43.0, \beta = 97.0$	$P2_1$	1.80	80	2.7	37	2vs2	Tuan *et al.* (2007), Coates *et al.* (2008)
Human deoxyhemoglobin (HbA)	$a = 63.8, b = 84.5, c = 54.4, \beta = 99.3$	$P2_1$	2.0	87	20	18	3kmf	Kovalevsky, Chatake *et al.* (2008, 2010)
XI–$2Mg^{2+}$–D-xylulose	$a = 94.6, b = 100.0, c = 104.0$	$I222$	2.2	89	4	37	3cwh	Kovalevsky, Katz *et al.* (2008)
HCA II	$a = 42.6, b = 41.6, c = 72.8, \beta = 104.6$	$P2_1$	2.0	85	1.2	55	3kkx	Fisher *et al.* (2009, 2010)
DFPase	$a = 43.3, b = 83.3, c = 87.5$	$P2_12_12_1$	2.2	82	0.43	37	3byc	Blum *et al.* (2009)
Amicyanin	$a = 28.5, b = 55.9, c = 27.2, \beta = 95.6$	$P2_1$	1.8	68	2.6	21	3l45	Sukumar *et al.* (2005, 2010)
XI–$2Ni^{2+}$–D-glucose	$a = 94.0, b = 99.7, c = 102.9$	$I222$	1.8	84	15	20	3kco	Kovalevsky, Hanson *et al.* (2010)
Equine CNmet hemoglobin	$a = 108.9, b = 63.2, c = 54.7, \beta = 110.8$	$C2$	2.0	80	10	28	—	Kovalevsky, Fisher *et al.* (2010)

detector in order to collect wavelength-resolved Laue patterns using time-of-flight (TOF) techniques. Data are collected efficiently and with good signal to noise using all of the available neutrons (with a wavelength range of ~0.7–7.0 Å) in the pulsed (20 Hz) white beam. This TOF approach has allowed data to be collected from crystals with smaller volumes and larger unit-cell dimensions than previously (Blum *et al.*, 2007) and has allowed neutron crystallography to expand beyond its traditional boundaries to address larger and more complex biological problems (Blakeley *et al.*, 2008). Importantly, it is complementary to the monochromatic and quasi-Laue approaches being developed at reactor sources, which also allow data to be collected rapidly from crystals with radically smaller volumes, but which are better optimized for different unit-cell dimensions and different levels of sample deuteration (Blakeley, 2009).

In addition to these methodological and technical innovations, another new aspect of the PCS user facility is the wide spectrum of support offered to users. It became clear from an early stage that scientists using the PCS found neutron macromolecular crystallography challenging at several stages of the process and that the chances of success are greatly increased if support is offered at all of these stages. Support from 'gene to structure' has become a guiding principle for the PCS user facility. The PCS not only offers open access to neutron beam time, but also actively supports and develops new methods in protein expression, deuteration, purification, robotic crystallization and the synthesis of substrates with stable isotopes and provides aid with data-reduction and structure-refinement software and comprehensive neutron structure analysis.

In this paper, we describe the current PCS user facility and illustrate its capabilities for determining neutron macromolecular structures with some selected examples from the user program.

2. Capabilities and user program

The design of the PCS, which has been described previously (Langan *et al.*, 2004), has allowed efficient data collection from crystals as small as 0.3 mm^3 (Bennett *et al.*, 2006) and with a unit-cell edge as large as 103 Å (Katz *et al.*, 2006), although it can allow the resolution of data out to d spacings of 1 Å and with lattice repeats of up to 180 Å. From Table 1, which lists recent macromolecular structures solved on the PCS, it can be seen that the average number of days required to collect a data set is 25 and that the average completeness and resolution of these data sets is 80% and 2.0 Å, respectively. Data sets can be collected at both room and low (100 K) temperatures. The PCS is operational for eight months of the year, during which around 100 d are made available to external users from all over the world through the LANSCE user program. Beam time is allocated through a peer-review system, which processes around 20 experimental proposals each year. The number of requested days of beam time is typically 2–3 times greater than the number of days available, as illustrated in Fig. 1.

3. User support from 'gene to structure'

Scientists wishing to use the PCS are offered support in several challenging aspects of neutron macromolecular crystallography, as discussed below. However, an important question before investing time and effort in a neutron study is whether or not it is likely to be successful. From experience, it has been found that deuterated samples for the PCS should exceed 0.3 mm^3 in volume, although smaller perdeuterated samples of 0.1 mm^3 are feasible. Recently, an empirical guideline for successful neutron structure determination on the PCS has been reported based on an analysis of previous neutron structures (Blum *et al.*, 2010). Briefly, in addition to

these crystal volume requirements, the X-ray diffraction limit for neutron samples should be better than 2.0 Å and preferably better than 1.5 Å. These guidelines have been adopted for the optimal allocation of beam time on the PCS.

Despite the advanced capabilities that have been made available with the PCS, a large disadvantage of neutron crystallography remains the relatively low flux of the neutron beam, which requires either large crystals or very long exposure times for smaller crystals in order to collect data to sufficient resolution and completeness. It can often be difficult to grow large crystals of biological macromolecules and we address this problem using two different approaches: (i) optimizing the expression and purification of large quantities of protein and the resulting crystal volumes and (ii) replacing hydrogen (H) by its isotope deuterium (D) in crystals, called deuteration, which greatly enhances their neutron scattering properties and allows smaller volumes to become practicable.

Several different (bacterial) protein-expression systems have been used for optimizing the production of protein (*e.g.* expression in hydrogenous or perdeuterated algae hydrolysate or minimal medium in deuterated water utilizing hydrogenous glucose) and the subsequent purification of large quantities of protein is carried out using ÄKTAprime plus and ÄKTA purifier systems (GE Healthcare). We have developed expertise in obtaining large crystals by utilizing a robotic Oryx8 crystallization system (Douglas Instruments). Oryx8 allows accurate and methodical scanning of the crystallization phase diagram for batch and sitting-drop crystallizations. Scientists frequently visit the PCS user facility several weeks prior to their allocated beam time in order to use this method to reveal the exact conditions for best growing large crystals of their particular protein. Using on-site crystallization capabilities also eliminates the problems associated with transporting valuable samples to the PCS.

Crystals can be deuterated either by vapour exchange or by soaking in D_2O mother liquor. This replaces H in water and also at labile positions in the protein. To substitute the remaining H atoms (which are covalently bound to carbon), called perdeuteration, requires gene expression in a perdeuterated growth medium. While straightforward in principle, protein-expression systems can be sensitive to both the replacement of H_2O by D_2O in the growth medium and the exact amount and types of perdeuterated nutrients used and can also require lengthy adaptation periods before substantial growth is achieved. At the PCS user facility an algae-based approach to perdeuteration is used which has been described previously (Liu *et al.*, 2007; Blum *et al.*, 2010). This procedure is relatively inexpensive, does not require extensive adaptation and results in protein perdeuteration levels of close to 100%. In cases when high perdeuteration is not necessary, proteins are expressed in minimal medium (containing M9 salts) made with hydrogenous glucose, generating ∼85% perdeuteration levels. Although the crystal volumes required for perdeuterated crystals at the PCS can be <30% of those of their corresponding hydrogenous counterparts, perdeuteration does not guarantee success, since crystals of the perdeuterated protein may be more difficult to grow or may diffract to lower resolution.

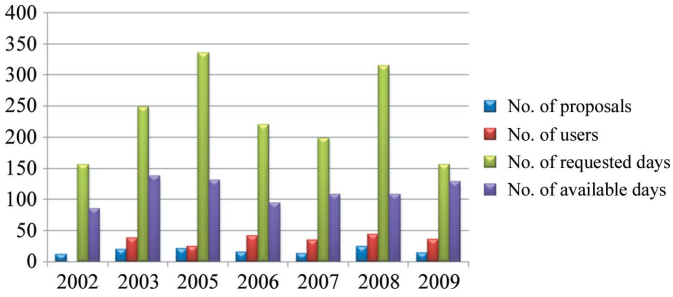

Figure 1
PCS user program statistics.

Data collection at the PCS can take several days/weeks and therefore usually involves scientists visiting at the start of an experiment to take part in mounting and screening samples and then, following their departure, a beamline scientist completing the data collection and processing. When a suitable crystal has been found, TOF wavelength-resolved Laue images are collected at several settings (depending on the space group) and these three-dimensional images are then processed using a version of *d*TREK* modified for TOF data (Langan & Greene, 2004). These processed data are then used for neutron structure refinement.

Until recently, neutron structure refinement was typically carried out separately from, and subsequent to, X-ray structure refinement, but was complicated for several reasons. In particular, it was common to modify existing X-ray programs to account for neutron data, which led to workable but non-optimal approaches for neutron refinement. At the same time, the increasing availability of both X-ray and neutron data provided an opportunity to develop a generalized method for structure analysis that exploits the complementarity of these data in order to provide more accurate and complete structures. These problems and opportunities were addressed by developing new tools for neutron structure refinement, *phenix.refine* and *nCNS*, which allow joint X-ray and neutron structure refinement, which we call XN refinement (Adams *et al.*, 2009; Afonine *et al.*, 2010). The *PHENIX* software, which is available from http://www.phenix-online.org, and the *nCNS* software, which is available from http://mnc.lanl.gov, are the results of an ongoing National Institutes of Health-funded collaboration between groups at Los Alamos and Lawrence Berkeley National Laboratories. These tools have been widely adopted by the international macromolecular neutron crystallography community.

4. Recent scientific highlights

Neutron crystallography is a powerful technique for locating H atoms and the PCS is typically used to provide information on the protonation states of amino-acid residues, the identity of solvent molecules and the nature of bonds involving hydrogen. The PCS can also be used to identify H atoms that are exchanged with D and the extent of this replacement, thus providing a tool for studying solvent accessibility and mole-

cular dynamics. Below, we present some selected highlights from the PCS user program that illustrate how the unique information provided by the PCS is being used to address important problems in biology, human health, renewable energy and the environment.

Endothiapepsin is an aspartic protease, a class of proteolytic enzymes that are widely distributed among life forms and viruses. Proteases are important drug targets for numerous diseases, including hypertension, malaria, amyloid diseases and AIDS. Coates *et al.* (2008) have determined a neutron crystal structure of endothiapepsin from *Endothia parasitica* in complex with an inhibitor containing a *gem*-diol difluoroethylene isostere. The XN structure determined using *nCNS* (Adams *et al.*, 2009) revealed that one of the two catalytic aspartic acid residues (Asp215) forming the active site was protonated on the outer oxygen of the carboxylate group and makes a strong hydrogen bond to one of the hydroxyls of the inhibitor. The other aspartate (Asp32) is deprotonated and accepts hydrogen bonds from both hydroxyls of the inhibitor. It has long been suggested that owing to the low pH optimum of the enzyme and the close proximity of the aspartic acids one of them has to be protonated; however, the location of this H in the *gem*-diol intermediate proposed to form after the substrate is attacked by the lytic water has been broadly disputed. This result provided the necessary direct evidence to settle this dispute and also suggested that the negative charge on Asp32 stabilizes the transition state; this is important information for the design of more effective aspartic protease inhibitors.

Tetrameric human hemoglobin (HbA) undergoes quaternary and tertiary structure changes during oxygen binding and release. Deoxygenated HbA (deoxy-HbA) has a low affinity for O_2 and its overall structure is referred to as the T (tense) state, while the oxygenated form is in the R (relaxed) state (Monod *et al.*, 1965; Perutz *et al.*, 1998; Yonetani *et al.*, 2002). The equilibrium between the T and R states is modulated by homotropic oxygen and heterotropic ions and small molecules, such as H^+, CO_2, Cl^- and phosphate. H^+ cations play a key role in the allosteric regulation of HbA, with deoxy-HbA having a higher affinity for H^+ than oxy-HbA. Thus, oxygen binding is dependent on pH, as demonstrated by the Bohr effect (Wyman, 1964). This implies the existence of H^+-binding sites (Bohr groups) that take up or release protons owing to their pK_a-value shifts during T↔R transitions (Perutz, 1970; Fang *et al.*, 1999). Knowledge of the protonation states of these residues is of great importance for better understanding how HbA functions. An international team led by Morimoto has determined the neutron structure of deoxy-HbA at 2 Å resolution, revealing the protonation states of 35 of a total of 38 His residues (Kovalevsky, Chatake *et al.*, 2008, 2010). Examples of how the protonation states were determined are shown in Fig. 2. Most importantly, the protonation states of the distal αHis58 and βHis63 and the buried αHis103 were directly determined using these data. On the basis of the protonation of the distal His residues in the $\alpha_1\beta_1$ heterodimer and of the buried His residues in both α chains and a comparison with a previous neutron analysis (Chatake *et al.*, 2007), the authors were able to propose the involvement of these residues in the Bohr effect. These residues have never before been considered as Bohr groups and their pK_a values and shifts have not been established (Fang *et al.*, 1999; Sun *et al.*, 1997). A surprising discovery was that seven pairs of His residues, αHis20, αHis50, αHis58, αHis89, βHis63, βHis143 and βHis146, from equivalent globin subunits showed different protonation states. For some, crystal packing could be a significant factor. For others, such as the distal His and the surface βHis143 and βHis146 residues, it is more likely that the $\alpha_2\beta_2$ heterodimer was no longer in the pure T state, while the deoxy-form structure was kept intact by the crystal forces.

Several enzymes that are important to DOE programs in renewable energy and the environment are being studied at the PCS with a view to understanding their detailed catalytic mechanisms. This new information is then being exploited to manipulate their performance and use. One such enzyme is D-xylose isomerase (XI). A major problem for the efficient use of cellulosic biomass in the production of biofuels is the presence of xylose in biomass hydrolyzates. Xylose is a pentose sugar which cannot be fermented by *Saccharomyces cerevisiae*. One pathway is the isomerization of xylose to xylulose by the expression of *xylA*, a gene found in some anaerobic fungi and bacteria that encodes XI. XI catalyzes the fully reversible sugar-conversion reaction between the aldo-sugars D-xylose and D-glucose and the keto-sugars D-xylulose and D-fructose, respectively. Glusker and coworkers have obtained a series of neutron structures of XI in complexes with different metals and substrates to generate snapshots of the sugar conversion at several stages of the reaction (Katz *et al.*, 2006; Kovalevsky, Katz *et al.*, 2008; Kovalevsky, Hanson *et al.*, 2010). The structures are of native XI with two Co^{2+} metal cofactors bound (XI-Co) and of complexes with Cd^{2+}

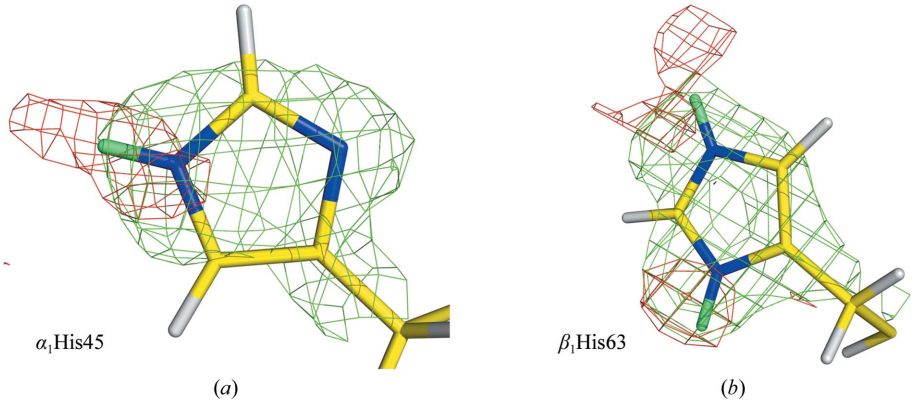

Figure 2
OMIT $F_o - F_c$ (red, contoured at the 2σ level) and $2F_o - F_c$ (green, contoured at the 1.6σ level) nuclear density maps for α_1His45 (*a*) and β_1His63 (*b*) residues that demonstrate how the protonation states for neutral and charged histidines, respectively, were determined. Peaks in OMIT $F_o - F_c$ maps correspond to D atoms.

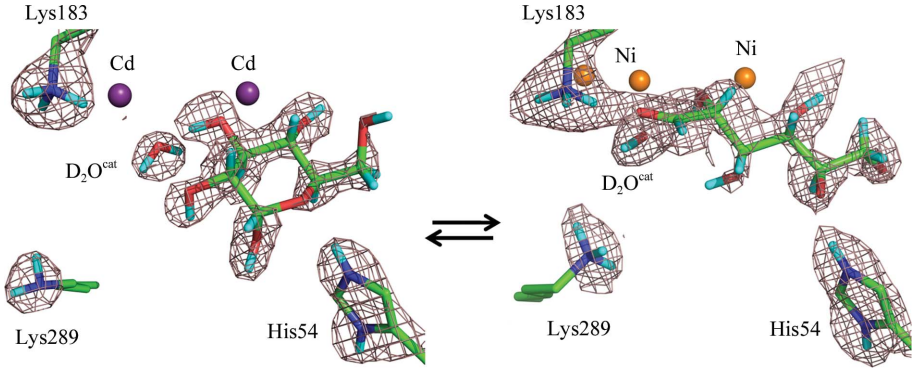

Figure 3
Cyclic and linear glucose substrates binding in XI-Cd-CyclicSugar and XI-Ni-LinearSugar, respectively, and the important active-site residues His54, Lys813 and Lys289. Neutron scattering density shown is contoured at the 1.6σ level.

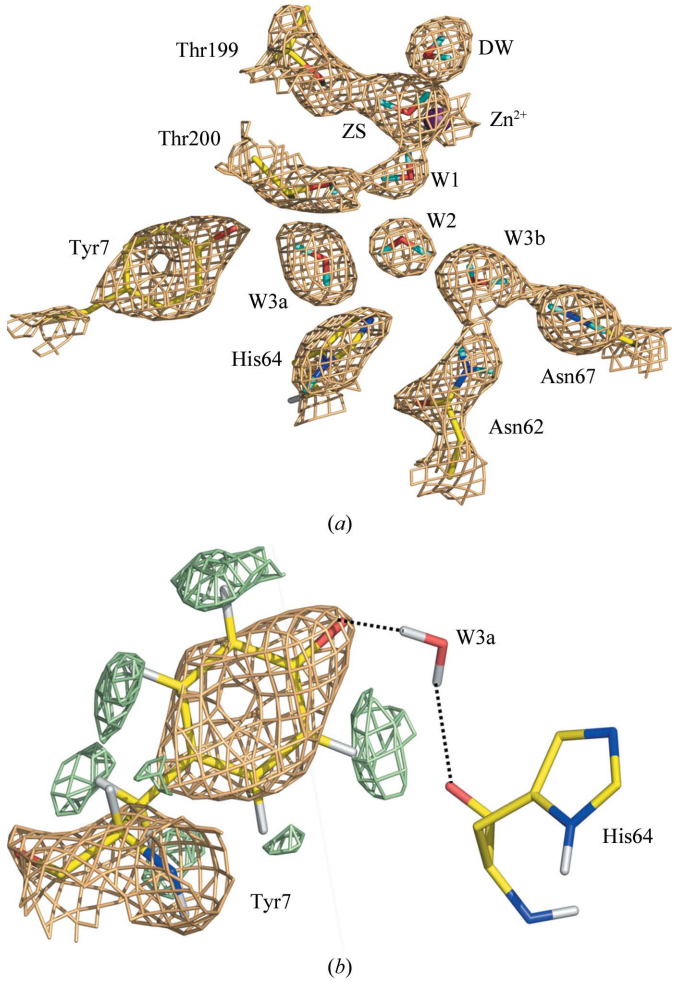

Figure 4
Neutron structure of HCA II. (*a*) Active-site residues and water network of HCA II shown in ball-and-stick representation; $2F_o - F_c$ nuclear map in orange, contoured at 1.5σ. (*b*) Tyr7 is deprotonated and is a hydrogen-bond acceptor of W3a; $2F_o - F_c$ positive nuclear map in orange, negative map in green, both contoured at 1.5σ.

cations and the substrate D-glucose-d_{14} (XI-Cd-CyclicSugar), with Ni^{2+} cations and the substrate linear D-glucose-d_{14} (XI-Ni-LinearSugar) and with Mg^{2+} cations and the product linear D-xylulose-d_{12} (XI-Mg-LinearProduct). The first structure with no sugar bound represents the reactant state, while the other three complexes correspond to the cyclic and linear substrate states and the linear product state, respectively. These results shed new light on the XI mechanism. The catalytic histidine His54 was found to be protonated at both the $N^{\delta1}$ and $N^{\varepsilon2}$ positions in all four neutron structures, suggesting that it does not permanently donate a proton to the O5 *endo*-cyclic sugar oxygen to promote the first ring-opening step, as previously proposed (Whitaker *et al.*, 1995). The O1 hydroxyl cannot donate its hydrogen to His54 during this reaction step, but rather may protonate a nearby water molecule which then passes it to Lys289 in a relay fashion. This proposal was corroborated by the finding that Lys289 is neutral (ND_2) in XI-Co and XI-Cd-CyclicSugar but is protonated (ND_3^+) in XI-Ni-LinearSugar (Fig. 3). Another important finding was that Lys183, which was previously thought to protonate O1 of the linear sugar during the isomerization step (Hu *et al.*, 1997), was protonated throughout the four neutron structures. The catalytic water (D_2O^{cat} in Fig. 3) is a water in XI-Co, XI-Cd-CyclicSugar and XI-Ni-LinearSugar but is converted to the hydroxide anion (OD^-) in XI-Mg-LinearProduct. Consequently, it was suggested that the catalytic water protonates O1, not Lys183. The Ni^{2+} cation coordinated with the D_2O^{cat} was observed in two distinct positions, with one closer to the linear substrate, which is in agreement with previous studies that demonstrated the mobility of this metal position and its possible role in aiding the isomerization step (Bogumil *et al.*, 1997; Fenn *et al.*, 2004). These observations do not support many aspects of the several proposals that have been advanced for the mechanism of XI. Rather, they lead to other possible mechanisms, which are being used to guide protein-engineering efforts.

Another enzyme with important applications in bioenergy and the environment is carbonic anhydrase (CA), a zinc metalloenzyme that catalyzes the reversible conversion of carbon dioxide to bicarbonate. CAs are being developed for enhanced algal growth and CO_2 capture. The reaction catalyzed by CA is rate-limited by a proton-transfer event between a Zn-bound water and the internal proton shuttle His64. This excess proton is transferred *via* a hydrogen-bonded water wire found between the catalytic Zn and bulk solvent. Despite the availability of numerous high-resolution X-ray structures of CA, several important active-site features have remained elusive. Specifically, the protonation state of the proton shuttle His64, the orientation and hydrogen-bonding interactions of active-site amino-acid residues with the water network and the identity of the catalytic metal-bound solvent species have not been elucidated. In order to reveal these features and determine how they pertain to catalysis, an XN study was initiated. Fisher *et al.* (2010) have reported the successful preparation of a large H/D-exchanged crystal (~1.2 mm^3) and the determination of the 2.0 Å XN structure of CA at the PCS. A detailed

analysis of the water wire, the protonation states of the hydrophilic residues that line the active site and their interaction with the water wire has been performed. Several novel and interesting aspects of the CA active site were discovered: (i) the Zn-bound solvent is a water molecule, not a hydroxide as previously thought, (ii) the water network appears to be broken, *i.e.* there is no direct hydrogen-bonded network leading from Zn to His64, (iii) His64 is neutral and has a single orientation, ready to accept an excess proton, and (iv) unexpectedly, Tyr7, a hydrophilic residue that hydrogen bonds to the water network, was found to be deprotonated, *i.e.* the phenolic hydroxyl has lost a proton and thus has a −1 charge. Fig. 4(*a*) shows the active site of HCA II, including the D atoms observed in the neutron structure. In Fig. 4(*b*) the deprotonated Tyr7 and its relation to the rest of the active site is depicted. These observations have implications for how proton transfer proceeds and the neutron structure provides a possible proton-transfer pathway that was not previously seen using conventional X-ray crystallographic techniques. This information will be used to re-engineer the enzyme for applications in biofuel production and carbon sequestration.

5. Conclusions

The PCS is an important proof-of-principle for the innovation of spallation macromolecular neutron crystallography and is a much-needed addition to the now growing pool of neutron beamlines available worldwide to the structural biology community. Its capabilities are complementary to those of macromolecular neutron beamlines being developed at reactor neutron sources and next-generation spallation neutron sources. A guiding principle for the PCS user facility has been to provide support at all stages of the process of a neutron crystallography study from gene to structure. Scientific results from the user program demonstrate how the PCS is being used to broaden the application of neutron crystallography to address a wide range of problems in biology, human health, renewable energy and the environment.

The PCS is funded by the Office of Biological and Environmental Research of the Department of Energy. MM and PL were partly supported by an NIH–NIGMS-funded consortium (1R01GM071939-01) between LANL and LNBL to develop computational tools for neutron protein crystallography. AYK was partly supported by a LANL LDRD grant (20080789PRD3). AYK and PL were partly supported by a LANL LDRD grant (20070131ER). HJ was supported by a University of California UCOP grant.

References

Adams, P. D., Mustyakimov, M., Afonine, P. V. & Langan, P. (2009). *Acta Cryst.* D**65**, 567–573.
Afonine, P. V., Mustyakimov, M., Grosse-Kunstleve, R. W., Moriarty, N. W., Langan, P. & Adams, P. D. (2010). *Acta Cryst.* D**66**, 1153–1163.
Bennett, B., Langan, P., Coates, L., Mustyakimov, M., Schoenborn, B., Howell, E. E. & Dealwis, C. (2006). *Proc. Natl Acad. Sci. USA*, **103**, 18493–18498.
Blakeley, M. P. (2009). *Crystallogr. Rev.* **15**, 157–218.
Blakeley, M. P., Langan, P., Niimura, N. & Podjarny, A. (2008). *Curr. Opin. Struct. Biol.* **18**, 593–600.
Blum, M.-M., Koglin, A., Rüterjans, H., Schoenborn, B., Langan, P. & Chen, J. C.-H. (2007). *Acta Cryst.* F**63**, 42–45.
Blum, M.-M., Mustyakimov, M., Rüterjans, H., Kehe, K., Schoenborn, B. P., Langan, P. & Chen, J. C.-H. (2009). *Proc. Natl Acad. Sci. USA*, **106**, 713–718.
Blum, M.-M., Tomanicek, S. J., John, H., Hanson, B. L., Rüterjans, H., Schoenborn, B. P., Langan, P. & Chen, J. C.-H. (2010). *Acta Cryst.* F**66**, 379–385.
Bogumil, R., Kappl, R., Hüttermann, J. & Witzel, H. (1997). *Biochemistry*, **36**, 2345–2352.
Chatake, T., Shibayama, N., Park, S.-Y., Kurihara, K., Tamada, T., Tanaka, I., Niimura, N., Kuroki, R. & Morimoto, Y. (2007). *J. Am. Chem. Soc.* **129**, 14840–14841.
Coates, L., Tuan, H.-F., Tomanicek, S., Kovalevsky, A., Mustyakimov, M., Erskine, P. & Cooper, J. (2008). *J. Am. Chem. Soc.* **130**, 7235–7237.
Fang, T.-Y., Zou, M., Simplaceanu, V., Ho, N. T. & Ho, C. (1999). *Biochemistry*, **38**, 13423–13432.
Fenn, T. D., Ringe, D. & Petsko, G. A. (2004). *Biochemistry*, **43**, 6464–6474.
Fisher, S. Z., Anderson, S., Henning, R., Moffat, K., Langan, P., Thiyagarajan, P. & Schultz, A. J. (2007). *Acta Cryst.* D**63**, 1178–1184.
Fisher, S. Z., Kovalevsky, A. Y., Domsic, J. F., Mustyakimov, M., McKenna, R., Silverman, D. N. & Langan, P. A. (2010). *Biochemistry*, **49**, 415–421.
Fisher, S. Z., Kovalevsky, A. Y., Domsic, J. F., Mustyakimov, M., Silverman, D. N., McKenna, R. & Langan, P. (2009). *Acta Cryst.* F**65**, 495–498.
Hu, H., Liu, H. & Shi, Y. (1997). *Proteins*, **27**, 545–555.
Katz, A. K., Li, X., Carrell, H. L., Hanson, B. L., Langan, P., Coates, L., Schoenborn, B. P., Glusker, J. P. & Bunick, G. J. (2006). *Proc. Natl Acad. Sci. USA*, **103**, 8342–8347.
Kovalevsky, A. Y., Chatake, T., Shibayama, N., Park, S.-Y., Ishikawa, T., Mustyakimov, M., Fisher, S. Z., Langan, P. & Morimoto, Y. (2008). *Acta Cryst.* F**64**, 270–273.
Kovalevsky, A. Y., Chatake, T., Shibayama, N., Park, S.-Y., Ishikawa, T., Mustyakimov, M., Fisher, Z., Langan, P. & Morimoto, Y. (2010). *J. Mol. Biol.* **398**, 276–291.
Kovalevsky, A. Y., Fisher, S. Z., Seaver, S., Mustyakimov, M., Sukumar, N., Langan, P., Mueser, T. C. & Hanson, B. L. (2010). *Acta Cryst.* F**66**, 474–477.
Kovalevsky, A. Y., Hanson, L., Fisher, S. Z., Mustyakimov, M., Mason, S., Forsyth, T., Blakeley, M. P., Keen, D. A., Wagner, T., Carrell, H. L., Katz, A. K., Glusker, J. P. & Langan, P. (2010). *Structure*, **18**, 688–699.
Kovalevsky, A. Y., Katz, A. K., Carrell, H. L., Hanson, L., Mustyakimov, M., Fisher, S. Z., Coates, L., Schoenborn, B. P., Bunick, G. J., Glusker, J. P. & Langan, P. (2008). *Biochemistry*, **47**, 7595–7597.
Langan, P. & Greene, G. (2004). *J. Appl. Cryst.* **37**, 253–257.
Langan, P., Greene, G. & Schoenborn, B. P. (2004). *J. Appl. Cryst.* **37**, 24–31.
Langan, P., Li, X., Hanson, B. L., Coates, L. & Mustyakimov, M. (2006). *Acta Cryst.* F**62**, 453–456.
Li, X., Langan, P., Bau, R., Tsyba, I., Jenney, F. E., Adams, M. W. W. & Schoenborn, B. P. (2004). *Acta Cryst.* D**60**, 200–202.
Liu, X., Hanson, B. L., Langan, P. & Viola, R. E. (2007). *Acta Cryst.* D**63**, 1000–1008.
Monod, J., Wyman, J. & Changeux, J.-P. (1965). *J. Mol. Biol.* **12**, 88–118.
Perutz, M. F. (1970). *Nature (London)*, **228**, 726–739.
Perutz, M. F., Wilkinson, A. J., Paoli, M. & Dodson, G. G. (1998). *Annu. Rev. Biophys. Struct.* **27**, 1–34.

Sukumar, N., Langan, P., Mathews, F. S., Jones, L. H., Thiyagarajan, P., Schoenborn, B. P. & Davidson, V. L. (2005). *Acta Cryst.* D**61**, 640–642.
Sukumar, N., Mathews, F. S., Langan, P. & Davidson, V. L. (2010). *Proc. Natl Acad. Sci. USA*, **107**, 6817–6822.
Sun, D. P., Zou, M., Ho, N. T. & Ho, C. (1997). *Biochemistry*, **36**, 6663–6673.
Teixeira, S. C. M. *et al.* (2008). *Chem. Phys.* **345**, 133–151.
Tuan, H.-F., Erskine, P., Langan, P., Cooper, J. & Coates, L. (2007). *Acta Cryst.* F**63**, 1080–1083.
Whitaker, R. D., Cho, Y., Cha, J., Carrell, H. L., Glusker, J. P., Karplus, P. A. & Batt, C. A. (1995). *J. Biol. Chem.* **270**, 22895–22906.
Wyman, J. (1964). *Adv. Protein Chem.* **19**, 223–286.
Yonetani, T., Park, S., Tsuneshige, A., Imai, K. & Kanaori, K. (2002). *J. Biol. Chem.* **277**, 34508–34520.